Role of the GALT in scrapie agent neuroinvasion from the intestine

THE JOURNAL OF IMMUNOLOGY

Role of the GALT in Scrapie Agent Neuroinvasion from the Intestine

Bridget R. Glaysher and Neil A. Mabbott

J Immunol 2007; 178:3757-3766; ;
http://www.jimmunol.org/content/178/6/3757

The Journal of Immunology is published twice each month by
The American Association of Immunologists, Inc.,
9650 Rockville Pike, Bethesda, MD 20814-3994.

Print ISSN: 0022-1767 Online ISSN: 1550-6606.

Role of the GALT in Scrapie Agent Neuroinvasion from the Intestine[1]

Bridget R. Glaysher and Neil A. Mabbott[2]

Following oral exposure, some transmissible spongiform encephalopathy (TSE) agents accumulate first upon follicular dendritic cells (FDCs) in the GALT. Studies in mice have shown that this accumulation is obligatory for the efficient delivery of the TSE agent to the brain. However, which GALTs are crucial for disease pathogenesis is uncertain. Mice deficient in specific GALT components were used here to determine their separate involvement in scrapie agent neuroinvasion from the intestine. In the combined absence of the GALTs and FDCs (lymphotoxin (LT)$\alpha^{-/-}$ mice and LT$\beta^{-/-}$ mice), scrapie agent transmission was blocked. When FDC maturation was induced in remaining lymphoid tissues, mice that lacked both Peyer's patches (PPs) and mesenteric lymph nodes (wild-type (WT)→LT$\alpha^{-/-}$ mice) or PPs alone (WT→LT$\beta^{-/-}$ mice) remained refractory to disease, demonstrating an important role for the PPs. Although early scrapie agent accumulation also occurs within the mesenteric lymph nodes, their presence in WT→LT$\beta^{-/-}$ mice did not restore disease susceptibility. We have also shown that isolated lymphoid follicles (ILFs) are important novel sites of TSE agent accumulation in the intestine. Mice that lacked PPs but contained numerous FDC-containing mature ILFs succumbed to scrapie at similar times to control mice. Because the formation and maturation status of ILFs is inducible and influenced by the gut flora, our data suggest that such factors could dramatically affect susceptibility to orally acquired TSE agents. In conclusion, these data demonstrate that following oral exposure TSE agent accumulation upon FDCs within lymphoid tissue within the intestine itself is critically required for efficient neuroinvasion. ***The Journal of Immunology,*** **2007, 178: 3757–3766.**

Transmissible spongiform encephalopathies (TSEs),[3] or "prion diseases," are subacute neurodegenerative diseases that affect humans and both domestic and free-ranging animals. The neuropathological features within the CNS characteristically include spongiform pathology, neuronal loss, glial activation, and amyloidal aggregations of an abnormally folded host protein. There is little evidence of pathology in other tissues. The host prion protein (PrP^c) is widely expressed in both humans and animals, and its expression is crucial for TSE disease susceptibility (1). In TSE-affected tissues, the PrP accumulates as an abnormal, detergent-insoluble, relatively proteinase-resistant isoform, termed PrP^{Sc}. TSE agent infectivity copurifies with PrP^{Sc} (2) and is considered to be a major or possibly sole component of the infectious TSE agent. Indeed, the prion hypothesis argues that PrP^{Sc} is itself the infectious agent and facilitates conversion of cellular PrP^c to PrP^{Sc}.

TSE diseases typically have long incubation periods before the onset of clinical signs, which in humans can vary from 1.5 to at least 40 years. Following peripheral exposure, many of the acquired TSE agents accumulate in lymphoid tissues such as the spleen, lymph nodes, tonsils, appendix, and Peyer's patches (PPs), before spreading to the CNS, a process termed neuroinvasion. Examples include sheep with natural scrapie (3), mule deer with chronic wasting disease (4), and humans with variant Creutzfeldt-Jakob disease (vCJD) (5). Within the lymphoid tissues of both experimentally and naturally affected hosts, early PrP^{Sc} accumulation occurs within the germinal centers upon follicular dendritic cells (FDCs) and within tingible body macrophages (4–9). FDCs are a distinct lineage from migratory bone marrow-derived dendritic cells because they are considered to derive from stromal precursor cells, are nonphagocytic, and are nonmigratory (10). In mouse scrapie models, mature FDCs are critical for scrapie agent accumulation in lymphoid tissues, and in their absence, neuroinvasion is significantly impaired (11–14). From the lymphoid tissues, translocation to the CNS occurs via the peripheral nervous system (15, 16).

The suggestion that consumption of bovine spongiform encephalopathy-contaminated meat products is the most likely cause of vCJD in humans (17) has focused attention on the gastrointestinal tract as an important portal of TSE entry. Following intragastric or oral inoculation of rodents with scrapie, infectivity and PrP^{Sc} accumulate first in PPs, mesenteric lymph nodes (MLNs), and ganglia of the enteric nervous system long before their detection in the CNS (18, 19). Natural sheep scrapie may also be acquired orally as PrP^{Sc} is detected in the GALT before detection within the CNS (6). Likewise, PrP^{Sc} is first detected in the GALT following experimental oral inoculation of mule deer fawns (*Odocoileus hemionus*) with chronic wasting disease (4). The detection of disease-specific PrP within the GALT of a human vCJD patient 8 mo before the onset of clinical signs is also consistent with the transmission of this disease by the oral route (5).

Institute for Animal Health, Edinburgh United Kingdom

Received for publication October 12, 2006. Accepted for publication December 26, 2006.

The costs of publication of this article were defrayed in part by the payment of page charges. This article must therefore be hereby marked *advertisement* in accordance with 18 U.S.C. Section 1734 solely to indicate this fact.

[1] This work was supported by Medical Research Council Grant G69/1867 and the Biotechnology and Biological Sciences Research Council.

[2] Address for correspondence and reprint requests to Dr. Neil A. Mabbott, Neuropathogenesis Unit, Institute for Animal Health, Ogston Building, West Mains Road, Edinburgh, U.K. E-mail address: neil.mabbott@bbsrc.ac.uk

[3] Abbreviations used in this paper: TSE, transmissible spongiform encephalopathy; FDC, follicular dendritic cell; GFAP, glial fibrillary acid protein; ILF, isolated lymphoid follicle; iILF, immature ILF; LT, lymphotoxin; LYVE-1, lymphatic vessel endothelial hyaluronic acid receptor-1; mILF, mature ILF; MLN, mesenteric lymph node; pAb, polyclonal Ab; PP, Peyer's patch; PrP, prion protein; vCJD, variant Creutzfeldt-Jakob disease; WT, wild type.

The GALT comprises chiefly of appendix, tonsils, PPs, MLNs, and ILFs, but which if any of these tissues are crucial for the oral pathogenesis of TSEs is unclear. Previous studies have used a variety of immunodeficient mouse lines to study the involvement of FDCs and PPs in oral scrapie pathogenesis, including TNF-$\alpha^{-/-}$ × lymphotoxin (LT)$\alpha^{-/-}$ mice, *aly/aly* mice, $\beta7^{-/-}$ mice, RAG-$1^{-/-}$ mice, and $\mu MT^{-/-}$ mice (20–22). However, the individual contributions of the deficiencies in lymphoid tissue, lymphoid tissue microarchitecture, or FDC development were not distinguished in the same mouse strains. In the current study, mouse models were created that lacked specific GALT components (PPs, MLNs, and ILFs) but had mature FDC networks in the remaining lymphoid tissues. The presence of FDCs in the remaining lymphoid tissues ensured that TSE agent accumulation could occur within these tissues if the missing tissues were not critical to disease pathogenesis. Using these mouse models, experiments were designed to address the following questions: first, whether TSE susceptibility is reduced in the absence lymphoid tissue within the intestine itself (e.g., PPs)? Second, whether neuroinvasion occurs from multiple sites such that the lack of one compartment (e.g., PPs) can be compensated for by the presence of another (e.g., MLNs)? Third, whether neuroninvasion can occur via other lymphoid tissues (e.g., spleen) in the absence of the GALT?

Materials and Methods

Mice

LT$\alpha^{-/-}$ mice (23) and LT$\beta^{-/-}$ mice (24) were obtained from B&K Universal and were maintained on a C57BL/6 background. Age- and sex-matched C57BL/6 mice were used as immunocompetent wild-type (WT) controls in studies using LT$\alpha^{-/-}$ mice and LT$\beta^{-/-}$ mice.

Gamma irradiation and bone marrow reconstitution

Bone marrow from the femurs and tibias of immunocompetent C57BL/6 WT mice was prepared as a single-cell suspension (3×10^7–4×10^7 viable cells/ml) in HBSS (Invitrogen Life Technologies). Recipient adult (6–8 wk old) LT$\alpha^{-/-}$ mice, LT$\beta^{-/-}$ mice, and C57BL/6 mice were gamma irradiated (950 rad) and 24 h later reconstituted with 0.1 ml of bone marrow by injection into the tail vein.

PP-deficient mice

To create progeny mice deficient in PPs, timed pregnant C57BL/Dk mice were given a single i.v. injection of 100 μg of a fusion protein containing the soluble LTβR domain linked to the Fc portion of human IgG1 (LTβR-Ig; Ref 25) on day 11.5 of gestation (26).

Scrapie agent inoculation

For oral inoculation mice were fed individual food pellets doused with 50 μl of a 1.0% (w/v) scrapie brain homogenate prepared from mice terminally affected with ME7 scrapie. Where indicated, separate groups of mice were inoculated by intracranial injection with 20 μl of a 1.0% (w/v) scrapie mouse brain homogenate (containing $\sim 1 \times 10^{4.5}$ ID_{50} units). Following challenge, animals were coded and assessed weekly for signs of clinical disease and killed at a standard clinical end point (27). Scrapie diagnosis was confirmed by histopathological assessment of vacuolation in the brain. Where indicated, some mice were sacrificed 70 days postchallenge, and small intestines, MLNs, and spleens taken for further analysis. For the construction of lesion profiles, vacuolar changes were scored in nine gray-matter areas of brain as described previously (28).

Immunohistochemical and immunofluorescent analysis

Spleens and MLNs were removed and snap-frozen at the temperature of liquid nitrogen. Small intestines from each mouse were divided into three roughly equal parts, gently squeezed to remove gut contents, coiled, embedded in Tissue-Tek OCT Compound (Bayer), and snap-frozen at the temperature of liquid nitrogen. Serial frozen sections (10 μm in thickness) were cut on a cryostat. FDCs were visualized by staining with mAb 8C12 to detect CR1 (CD35) or mAb 7G6 to detect CR2/CR1 (CD21/CD35; BD Biosciences Pharmingen). Complement components C3 and C4 were detected using mAb RMC7H8 (Connex) and mAb FDC-M2 (AMS Biotechnology), respectively. Cellular PrP^c was detected using PrP-specific polyclonal Ab (pAb) 1B3 (29). B lymphocytes were detected using mAb B220 to detect CD45R (Caltag Laboratories). M cells were detected using biotin-conjugated *Ulex europaeus* agglutinin I (UEA-1; Vector Laboratories). Lymphatic vessels were detected using lymphatic vessel endothelial hyaluronic acid receptor (LYVE-1)-specific antiserum (Upstate Biotechnology). Nerve fibers and supportive cells were detected using S100-specific antiserum (DakoCytomation).

For the detection of disease-specific PrP (PrP^d) in brain tissue and small intestines, tissues were fixed in periodate-lysine-paraformaldehyde and embedded in paraffin wax. Sections (thickness, 6 μm) were deparaffinized and pretreated to enhance PrP immunostaining by hydrated autoclaving (15 min, 121°C, hydration), and subsequent immersion in formic acid (98%) for 5 min (7). This pretreatment enhances the detection of PrP^d. Sections were then stained with the PrP-specific pAb 1B3 (29). Glial fibrillary acid protein (GFAP) was detected on adjacent brain sections using rabbit GFAP-specific antiserum (DakoCytomation). To detect FDCs and B lymphocytes in paraffin-embedded small intestines, sections were deparaffinized and pretreated with Target Retrieval Solution (DakoCytomation) and immunostained with mAb 7G6 and mAb B220, respectively, as described above.

For light microscopy, following the addition of primary Abs, biotin-conjugated species-specific secondary Abs (Stratech) were applied followed by alkaline phosphatase or HRP coupled to the avidin/biotin complex (Vector Laboratories). Vector Red (Vector Laboratories) and diaminobenzidine were used as substrates, respectively, and sections were counterstained with hematoxylin to distinguish cell nuclei. For fluorescent microscopy, following the addition of primary Ab, species-specific secondary Abs coupled to Alexa Fluor 488 (green) or Alexa Fluor 594 (red) dyes (Invitrogen Life Technologies) were used. Sections were mounted in fluorescent mounting medium (DakoCytomation) and examined using a Zeiss LSM5 confocal microscope (Zeiss).

ILF enumeration and analysis

Entire small intestines from each mouse were divided into three equal parts, coiled, fixed in paraformaldehyde, and embedded in paraffin wax. Serial sections (10 μm in thickness) were deparaffinized and immunostained with antisera specific for CD45R or CR2/CR1 as described above and examined using a confocal microscope. The total number of B lymphocyte-containing ILFs in the entire small intestine of each mouse analyzed was counted microscopically using CD45R expression for identification. The maturity of each ILF was determined according to size and the location and density of component cells as described previously (30). The presence or absence of FDCs ($CR2/CR1^+CD45R^-$ cells) within each ILF was recorded.

Immunoblot detection of PrP^{Sc}

Spleen fragments (~20 mg) or MLNs (approximately half the total from each mouse assayed) were prepared as 10% (w/v) tissue homogenates, and PrP^{Sc} was enriched by sodium phosphotungstic acid precipitation (31) and treated in the presence or absence of proteinase K (40 μg/ml, 60 min, 37°C; VWR). Following enrichment, pellets were resuspended and diluted to 0.5 mg protein/ml, and 10 μl was electrophoresed through SDS-PAGE gels (12%) polyacrylamide gels (Invitrogen Life Technologies). Proteins were transferred to polyvinylidene difluoride membranes (Bio-Rad) by semidry blotting. PrP was detected with the PrP-specific mouse mAb 8H4 (32), followed by HRP-conjugated goat anti-mouse antiserum. Bound HRP activity was detected with Supersignal West Dura Extended Duration Substrate (Pierce).

Statistical analysis

Data are presented as mean ± SE. Significant differences between samples in different groups were sought by one-way ANOVA. Values of $p < 0.05$ were accepted as significant.

Results

Effect of lymphotoxin deficiency on scrapie accumulation in lymphoid tissues

The intestines of LT$\alpha^{-/-}$ mice and LT$\beta^{-/-}$ mice lack PPs as LTβR signaling during embryonic development is required for their formation (30, 33, 34). In addition LT$\alpha^{-/-}$ mice also lack the MLNs as LTα deficiency blocks their formation (34). However,

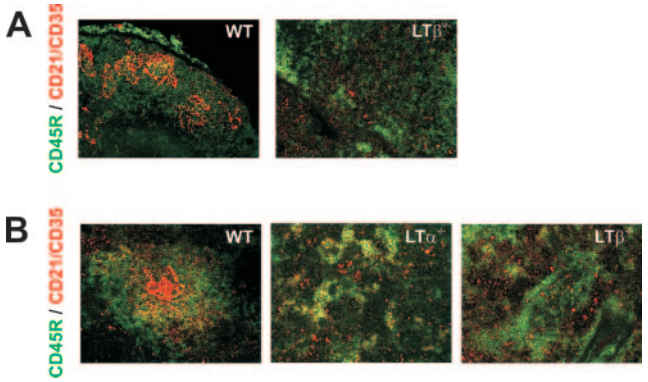

FIGURE 1. Immunohistochemical detection of FDCs within the MLNs (*A*) and spleens (*B*) of WT mice, LT$\alpha^{-/-}$ mice, and LT$\beta^{-/-}$ mice. CD21/CD35-expressing (red) FDCs and organized B lymphocyte follicles (CD45R-positive cells; green) were detected in the tissues of WT mice. No FDCs were detected in tissues from LT$\alpha^{-/-}$ mice and LT$\beta^{-/-}$ mice. Original magnification: ×200.

postnatal stimulation via lymphocyte-derived LT$\alpha_1\beta_2$ is critically required to maintain FDCs in their differentiated state (35). As a consequence, the remaining MLNs and spleens of LT$\beta^{-/-}$ mice (Fig. 1, *A* and *B*, respectively) and the spleens of LT$\alpha^{-/-}$ mice (Fig. 1*B*) are deficient in FDCs. Because FDCs are critical for the efficient neuroinvasion of the ME7 scrapie agent from the intestine (13), we first investigated scrapie pathogenesis in the combined absence of GALT (MLNs and/or PPs) and FDCs in the remaining lymphoid tissues in LT$\alpha^{-/-}$ mice and LT$\beta^{-/-}$ mice.

In this study, the normal cellular form of the PrP is referred to as PrP^{c}, and two terms (PrP^{Sc} or PrP^{d}) are used to describe the disease-specific, abnormal accumulations of PrP that are characteristically found only in TSE-affected tissues and considered to represent the presence of the TSE agent (2). Disease-specific PrP accumulations are relatively resistant to proteinase digestion, whereas cellular PrP^{c} is destroyed by this treatment. Where we were able to confirm this resistance by proteinase K treatment of samples and analysis by immunoblot, PrP^{Sc} is used as a biochemical marker for the presence of the TSE agent. Unfortunately, treatment of tissue sections with proteinase K destroys the microarchitecture. Therefore, tissue sections were fixed and pretreated to enhance the detection of the disease-specific abnormal accumulations of PrP (PrP^{d}), whereas cellular PrP^{c} is denatured by these treatments (7). We have shown in a series of studies that these PrP^{d} accumulations occur only in the tissues of TSE-affected animals and correlate closely with the presence of the TSE agent (7, 8, 11, 13, 19). Expression levels of cellular PrP^{c} in tissues from uninfected mice were analyzed on acetone-fixed frozen sections. Immunocompetent C57BL/6 WT mice, LT$\alpha^{-/-}$ mice, and LT$\beta^{-/-}$ mice were inoculated orally with the ME7 scrapie strain. Within 70 days of oral inoculation of WT mice with the ME7 scrapie agent, strong accumulations of PrP^{d} and agent infectivity are found within PPs (Ref. 13; N. A. Mabbott, unpublished observations). High levels of proteinase K-resistant PrP^{Sc} and agent infectivity are also found within MLNs (Fig. 2*A*, *lanes 2* and *4*; Ref. 13; N. A. Mabbott, unpublished observations) and are sustained until the terminal stage of disease (Fig. 2*C*, *lanes 2* and *4*). However, in the MLNs of LT$\beta^{-/-}$ mice or the mesenteric membranes taken from MLN-deficient LT$\alpha^{-/-}$ mice, PrP^{Sc} was undetectable both 70 days (Fig. 2*A*) and 545 days (Fig. 2*C*) after inoculation. No PrP^{Sc} was detected in any of the spleens from WT mice, LT$\alpha^{-/-}$ mice, and LT$\beta^{-/-}$ mice assayed 70 days after inoculation (Fig. 2*B*). However, strong accumulations of PrP^{Sc} were found in the spleens of WT mice taken at the terminal stage of disease (Fig. 2*D*), but the subsequent accumulation in the spleens of LT$\alpha^{-/-}$ mice and LT$\beta^{-/-}$ mice was blocked (Fig. 2*D*). Thus, in the absence of PPs and FDCs in remaining lymphoid tissues, PrP^{Sc} accumulation in MLNs and the spleen is blocked.

Effect of lymphotoxin deficiency on scrapie susceptibility

We next determined the effect of the combined GALT and FDC deficiency in LT$\alpha^{-/-}$ mice and LT$\beta^{-/-}$ mice on scrapie susceptibility. All orally inoculated WT mice succumbed to clinical TSE disease with a mean incubation period of 311 ± 3 days (n = 20; Table I). In contrast, LT deficiency dramatically affected scrapie-susceptibility as all LT$\alpha^{-/-}$ mice (n = 13) and LT$\beta^{-/-}$ mice (n = 18) remained free of the signs of scrapie up to at least 545 days after oral inoculation (Table I). Characteristic PrP^{d} accumulation, reactive astrocytes, and spongiform pathology were detected in the brains of all clinically affected WT mice (Fig. 3*A*). The severity and distribution of the pathological vacuolation within the brains of WT mice was typical for oral infection with the ME7 scrapie strain (Fig. 3*B*). However, none of the pathological

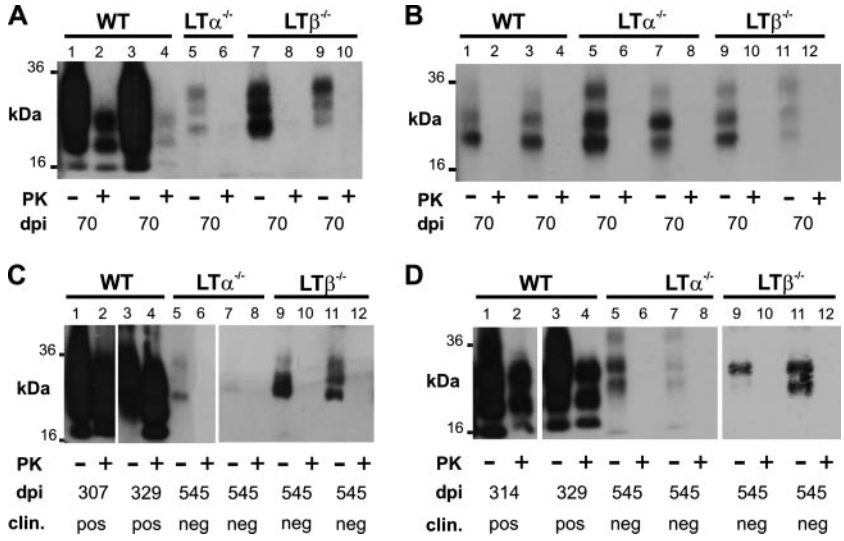

FIGURE 2. PrP^{Sc} accumulation in the MLNs and spleens of LT$\alpha^{-/-}$ mice and LT$\beta^{-/-}$ mice is blocked following oral inoculation with scrapie. *A* and *C*, MLNs (or the mesenteric membrane containing the region where MLNs would have been in LT$\alpha^{-/-}$ mice) and spleens (*B* and *D*) were collected 70 days after oral inoculation with the scrapie agent (*A* and *B*) or at the terminal stage of disease (*C* and *D*). Samples were treated in the presence (+) or absence (−) of proteinase K (PK) before electrophoresis. After PK treatment, a typical three-band pattern was observed between molecular mass values of 20–30 kDa, representing unglycosylated, monoglycosylated, and diglycosylated isomers of PrP (in order of increasing molecular mass). dpi, day postinoculation on which the tissues were analyzed; pos, mice that developed clinical signs of scrapie; neg, mice that were free of the signs of scrapie.

Table I. *Effect of lymphotoxin deficiency on scrapie agent susceptibility*

Mouse Strain	Presence at Time of Inoculation					Oral Inoculation		Intracranial Inoculation	
	PPs	mILFs[a]	MLNs	SPL	FDCs	Incidence[b]	Mean incubation period (days) ± SE	Incidence	Mean incubation period (days) ± SE
WT	+[c]	5	+	+	+	20/20	311 ± 3	6/6	173 ± 4
LTα$^{-/-}$	−	0	−	+	−	0/13	13X > 545	5/5	175 ± 4
LTβ$^{-/-}$	−	0	+	+	−	0/18	18X > 545	6/6	172 ± 3

[a] Number of mILFs present in the small intestine at the time of inoculation.
[b] Incidence = number of animals affected/number of animals tested. The notation "NX > 545" means that mice were free of the clinical and pathological signs of scrapie up to at least this time after inoculation.
[c] +, present; −, absent.

characteristics of TSE disease were detected within the brains of any of the surviving LTα$^{-/-}$ mice and LTβ$^{-/-}$ mice (Fig. 3, *A* and *B*).

When inoculated with the scrapie agent directly into the CNS (by intracranial injection) WT mice, LTα$^{-/-}$ mice, and LTβ$^{-/-}$ mice developed clinical scrapie with similar incubation periods of 172–175 days (Table I). These data confirm that the apparent resistance of LTα$^{-/-}$ mice and LTβ$^{-/-}$ mice to orally inoculated scrapie agent could not be attributed to a role for LTβR signaling in the development of pathology within the CNS.

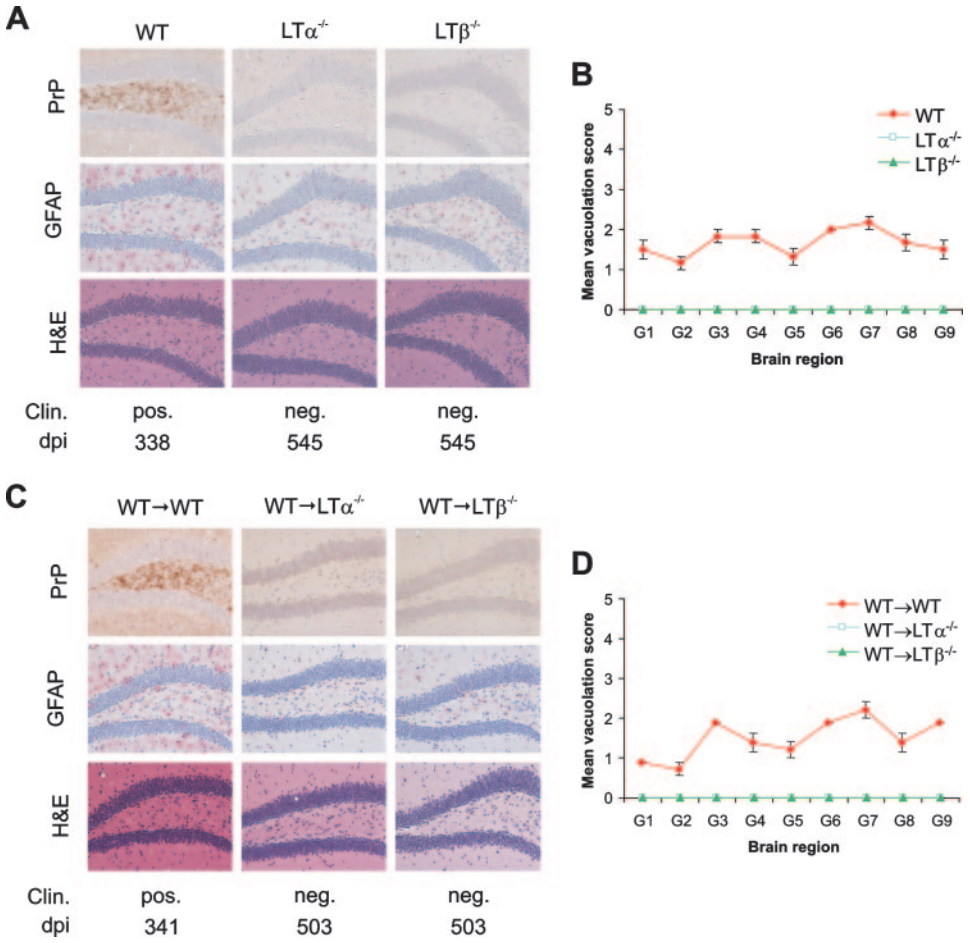

FIGURE 3. Immunohistochemical and pathological analysis of brain tissue from terminally scrapie-affected mice and mice that remained free of the signs of disease at the end of the experiment. *A* and *B*, Brains from WT mice, LTα$^{-/-}$ mice, and LTβ$^{-/-}$ mice inoculated orally with the scrapie agent. *C* and *D*, Brains from WT→WT mice, WT→LTα$^{-/-}$ mice, and WT→LTβ$^{-/-}$ mice inoculated orally with the scrapie agent. Large PrP^{d} accumulations (brown; *upper rows*), reactive astrocytes expressing high levels of GFAP (red; *middle rows*), and spongiform pathology (*lower rows*) were detected in the hippocampi of all clinically scrapie-affected WT mice (*A*) and WT→WT mice (*C*), but not in the brains clinically negative LTα$^{-/-}$ mice and LTβ$^{-/-}$ mice (*A*), and WT→LTα$^{-/-}$ mice and WT→LTβ$^{-/-}$ mice (*C*). All sections were counterstained with hematoxylin (blue). Original magnification: ×200. dpi, day postinoculation on which the tissues were analyzed; pos, mice that developed clinical signs of scrapie; neg, mice that were free of the signs of scrapie. *B* and *D*, Pathological assessment of the spongiform change (vacuolation) in brains from terminally scrapie-affected mice and mice that remained free of the signs of disease at the end of the experiment. Vacuolation was scored on a scale of 0–5 in the following gray matter (G1–G9) areas: G1, dorsal medulla; G2, cerebellar cortex; G3, superior colliculus; G4, hypothalamus; G5, thalamus; G6, hippocampus; G7, septum; G8, retrosplenial and adjacent motor cortex; G9, cingulate and adjacent motor cortex. Each point represents mean vacuolation score ± SE for groups of 6–20 mice.

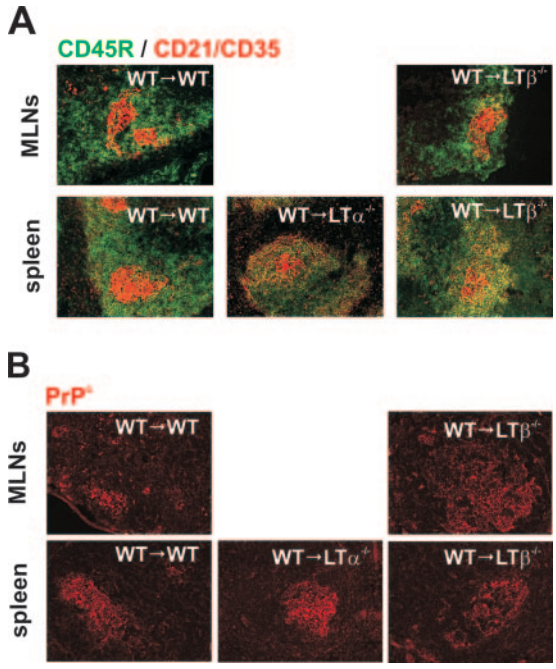

FIGURE 4. Immunohistochemical analysis of the microarchitecture of the MLNs and spleen at the time of scrapie challenge. *A*, CD21/CD35-expressing (red) FDCs and organized B lymphocyte follicles (CD45R-positive cells; green) were detected in the MLNs of WT→WT mice and WT→LT$\beta^{-/-}$ mice (*upper row*) and spleens of WT→WT mice, WT→LT$\alpha^{-/-}$ mice, and WT→LT$\beta^{-/-}$ mice (*lower row*). *B*, The levels of PrP^c expressed upon FDCs (red) were similar in the MLNs of WT→WT mice and WT→LT$\beta^{-/-}$ mice (*upper row*) and spleens of WT→WT mice, WT→LT$\alpha^{-/-}$ mice, and WT→LT$\beta^{-/-}$ mice (*lower row*). Original magnification: ×200.

Reconstitution of LT-deficient mice with WT bone marrow induces FDC development in remaining lymphoid tissues but not the development of missing lymphoid tissues

Next, the effects of GALT deficiency, but not FDC deficiency, on scrapie pathogenesis were investigated. Adult WT mice, LT$\alpha^{-/-}$ mice, and LT$\beta^{-/-}$ mice were reconstituted with LT-expressing WT bone marrow (termed WT→WT mice, WT→LT$\alpha^{-/-}$ mice, and WT→LT$\beta^{-/-}$ mice, respectively). Within 35 days of WT bone marrow transfer, FDC networks were induced in the remaining lymphoid tissues of LT$\alpha^{-/-}$ mice and LT$\beta^{-/-}$ mice (Fig. 4*A*), but such treatment did not induce the development of missing lymphoid tissues (Table II). Expression of the cellular form of the PrP, PrP^c, upon FDCs within the MLNs (where present) and spleens of WT→LT$\alpha^{-/-}$ mice and WT→LT$\beta^{-/-}$ mice appeared similar to that in tissues from WT→WT mice (Fig. 4*B*).

Scrapie pathogenesis in the absence of MLNs and/or PPs

Groups of WT→WT mice, WT→LT$\alpha^{-/-}$ mice, and WT→LT$\beta^{-/-}$ mice were inoculated orally with scrapie 35 days after reconstitution with WT bone marrow. Strong accumulations of PrP^d were observed within the PPs of WT→WT mice within 70 days of inoculation (Fig. 5*A*) and were maintained until the terminal stage of disease (Fig. 5*B*). The distribution of the PrP^d within PPs was consistent with accumulation upon FDCs (8, 13). However, PrP^d accumulation within the intestines of WT→LT$\alpha^{-/-}$ mice and WT→LT$\beta^{-/-}$ mice was blocked (Fig. 5).

In the MLNs, PrP^{Sc} was undetectable in tissues from WT→WT mice, WT→LT$\alpha^{-/-}$ mice, and WT→LT$\beta^{-/-}$ mice assayed 70 days after inoculation (Fig. 6*A*), although PrP^{Sc} was detected in one of the spleens from a WT→WT mice taken at this time (Fig. 6*B*, *lane 2*). At the terminal stage of disease strong accumulations of PrP^{Sc} were found in the MLNs and spleens of WT→WT mice (Fig. 6, *C* and *D*). However, the accumulation of PrP^{Sc} in the MLNs (where present) and spleens of WT→LT$\alpha^{-/-}$ mice and WT→LT$\beta^{-/-}$ mice remained undetectable (Fig. 6, *C* and *D*).

We next determined the effect of MLN and/or PP deficiency on disease susceptibility. All orally inoculated WT→WT mice succumbed to clinical TSE disease with a mean incubation period of 337 ± 4 days ($n = 8$, Table II). In contrast, in the absence of both PPs and MLNs, scrapie susceptibility was dramatically affected as all orally inoculated WT→LT$\alpha^{-/-}$ mice ($n = 8$) remained free of the signs of scrapie up to at least 503 days after inoculation (Table II). Furthermore, in the absence of PPs alone, scrapie susceptibility was also dramatically affected as all WT→LT$\beta^{-/-}$ mice ($n = 7$) remained free of clinical scrapie (Table II). Typical neuropathological characteristics of TSE infection were detected within the brains of all WT→WT animals that developed clinical signs of scrapie (Fig. 3, *C* and *D*). None of these characteristics were detected within the brains of any of the surviving WT→LT$\alpha^{-/-}$ mice and WT→LT$\beta^{-/-}$ mice (Fig. 3, *C* and *D*).

In this study, a highly sensitive immunoblot method was used to detect PrP^{Sc} in our tissue samples (31). Therefore, we are confident that in this study the combined absence of 1) PrP^{Sc} in the GALT and spleen, 2) PrP^d and neuropathological signs within the CNS, and 3) clinical signs of TSE disease, is convincing evidence that transmission was blocked in scrapie-inoculated LT$\alpha^{-/-}$ mice, LT$\beta^{-/-}$ mice, WT→LT$\alpha^{-/-}$ mice, and WT→LT$\beta^{-/-}$ mice.

Table II. *Reconstitution of LT-deficient mice with WT bone marrow induces FDC maturation in remaining lymphoid tissues but does not restore susceptibility to orally inoculated scrapie agent*

	Presence at Time of Inoculation					Oral Scrapie Inoculation	
Mouse Strain[a]	PPs	mILFs[b]	MLNs	SPL	FDCs	Incidence	Mean incubation period (days) ± SE
WT→WT	+[c]	0	+	+	+	8/8	337 ± 4
WT→LT$\alpha^{-/-}$	−	0	−	+	+	0/8	5X > 503[d]
WT→LT$\beta^{-/-}$	−	0	+	+	+	0/7	4X > 503[e]

[a] Mice were inoculated orally with the scrapie agent 35 days after gamma irradiation and reconstitution with WT bone marrow.

[b] Number of mILFs present in the small intestine at the time of inoculation.

[c] +, present; −, absent.

[d] Three mice were killed 406, 450, and 467 days after inoculation. These mice were free of the clinical signs of scrapie at the time of cull. No histopathological signs of scrapie were detected in the brain (data not shown).

[e] Three mice were killed 413, 455, and 455 days after inoculation. These mice were free of the clinical signs of scrapie at the time of cull. No histopathological signs of scrapie were detected in the brain (data not shown).

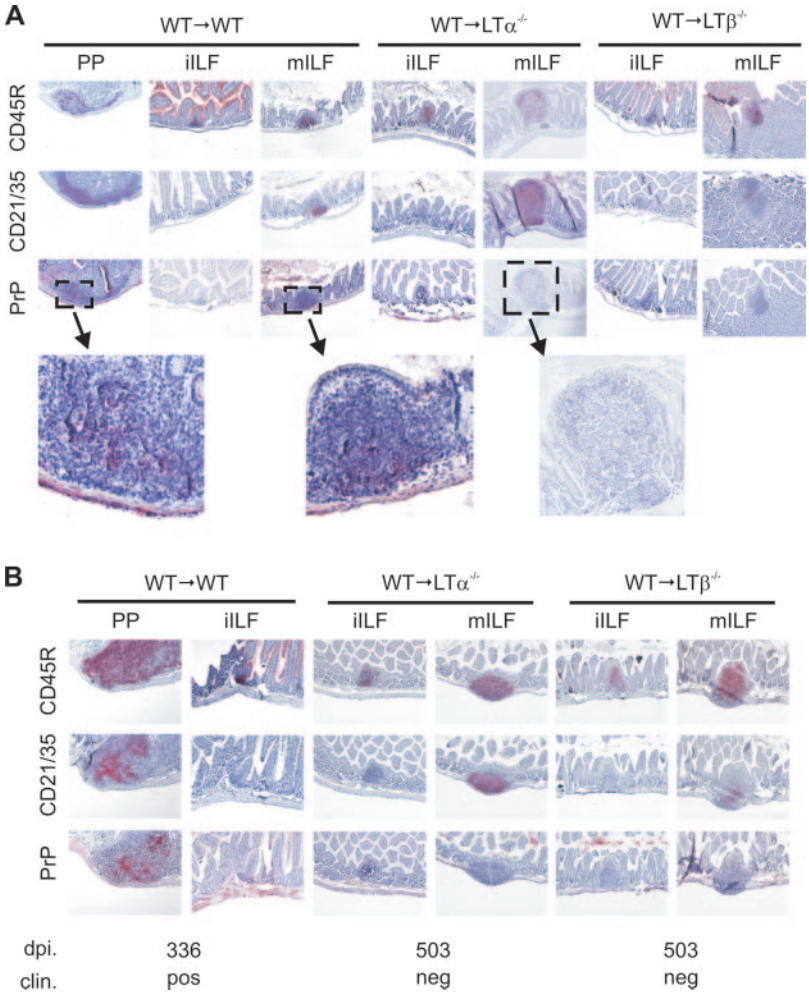

FIGURE 5. Detection of PrP^d in the intestines of WT→WT mice, WT→LT$\alpha^{-/-}$ mice, and WT→LT$\beta^{-/-}$ mice following oral inoculation with the scrapie agent. Small intestines were collected (*A*) 70 days after oral inoculation or (*B*) at the terminal stage of disease. Adjacent sections were stained with CD45R-specific antiserum B220 to detect B lymphocytes (red), CD21/35-specific antiserum to detect CR2/CR1-expressing FDCs (red), and PrP-specific antiserum 1B3 (red). Strong PrP^d staining colocalized with CD21/35 expressing FDCs in the PPs and the few mILFs of WT→WT mice 70 days after oral inoculation (*A*) and at the terminal stage of disease (*B*). PrP^d was not detected in the mILFs of scrapie-inoculated WT→LT$\alpha^{-/-}$ mice or WT→LT$\beta^{-/-}$ mice. dpi, day postinoculation on which the tissues were analyzed; pos, mice that developed clinical signs of scrapie; neg, mice that were free of the signs of scrapie. Original magnification: ×100.

Mature ILFs contain FDCs

Novel lymphoid clusters termed ILFs have been identified along the antimesenteric wall of the mucosa of the intestine (36). The maturity of ILFs has previously been defined according size and the location and density of component cells (30). Whereas immature ILFs (iILFs) comprise loosely clustered $CD45R^+$ (B220) cells located at the base of villi (Fig. 7*A*), mature ILFs (mILFs) are organized nodular structures, of width greater than one villus and comprise a single B lymphocyte follicle (Fig. 7*A*) with an overlying M cell-containing epithelium similar to the follicle associated epithelium of PPs (Fig. 7*D*). Using these criteria, double immunostaining for B lymphocytes ($CD45R^+$ cells) and FDCs ($CR2/CR1^+CD45R^-$ cells) on the same tissue section revealed that the presence of FDCs could also be reliably used to distinguish ILF

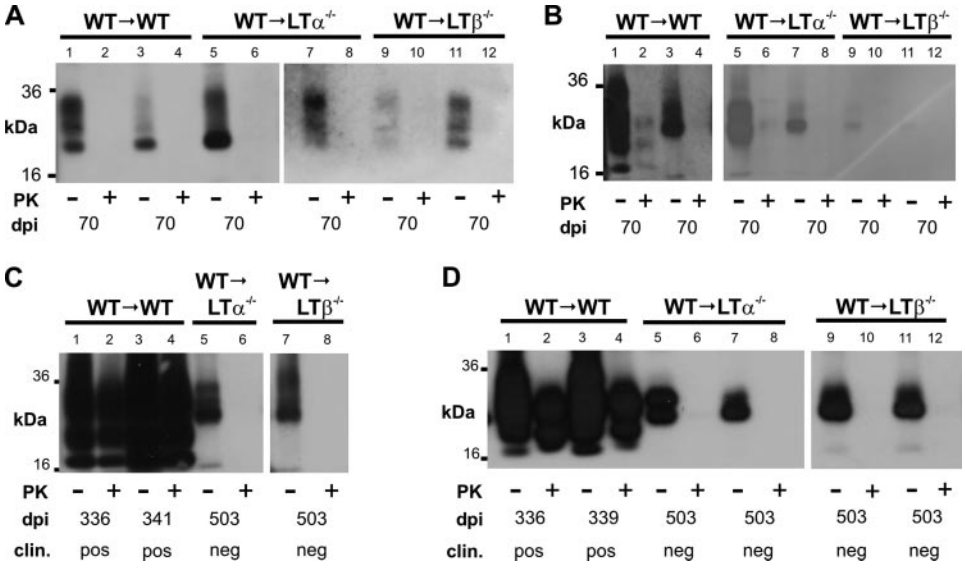

FIGURE 6. PrP^{Sc} accumulation in the MLNs and spleens of WT→LT$\alpha^{-/-}$ mice and WT→LT$\beta^{-/-}$ mice is blocked following oral inoculation with the scrapie agent. *A* and *C*, MLNs (or the mesenteric membrane containing the region where MLNs would have been in WT→LT$\alpha^{-/-}$ mice) and spleens (*B* and *D*) were collected 70 days after oral inoculation with the scrapie agent (*A* and *B*) or at the terminal stage of disease (*C* and *D*). Samples were treated in the presence (+) or absence (−) of proteinase K (PK) before electrophoresis. dpi, day postinoculation on which the tissues were analyzed; pos, mice that developed clinical signs of scrapie; neg, mice that were free of the signs of scrapie.

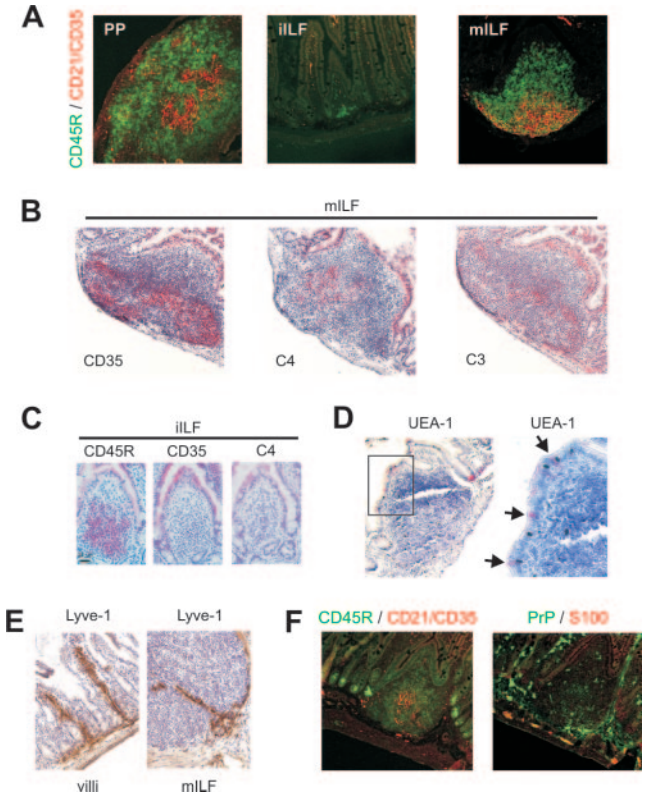

FIGURE 7. Immunohistochemical characterization of mILFs. *A*, iILFs typically comprise a loose aggregation of B lymphocytes at the base of a villus (CD45R-positive cells; green), whereas mILFs contain both B lymphocytes and CR2/CR1-expressing FDCs (CD21/CD35-positive cells; red). *B*, Complement components C4 (red; *middle*) and C3 (red; *right*) in association with CR1-expressing FDCs (CD35-positive cells; red; *left*) were detected within mILFs indicating the presence of functional FDCs. (*C*) In iILFs, CR1-expressing FDCs (CD35-positive cells; red; *middle*) and associated C4 (red; *right*) are absent. *D*, M cells (UEA-1-positive cells; red; arrowheads) were detected within the epithelium overlying mILFs. *Right panel* shows an enlargement of the boxed area. *E*, Lymphatic vessels (LYVE-1-expressing cells; brown) were detected within the cores of villi (*left panel*) and within and around mILFs (*right panel*). *F*, PrP (green) and S-100 (red)-expressing nerve fibers, and supportive cells were detected within the gut wall and in close association with mILFs. In *B–E*, sections were counterstained with hematoxylin (blue). Each image is orientated such that the intestinal lumen is uppermost. Original magnification: ×200.

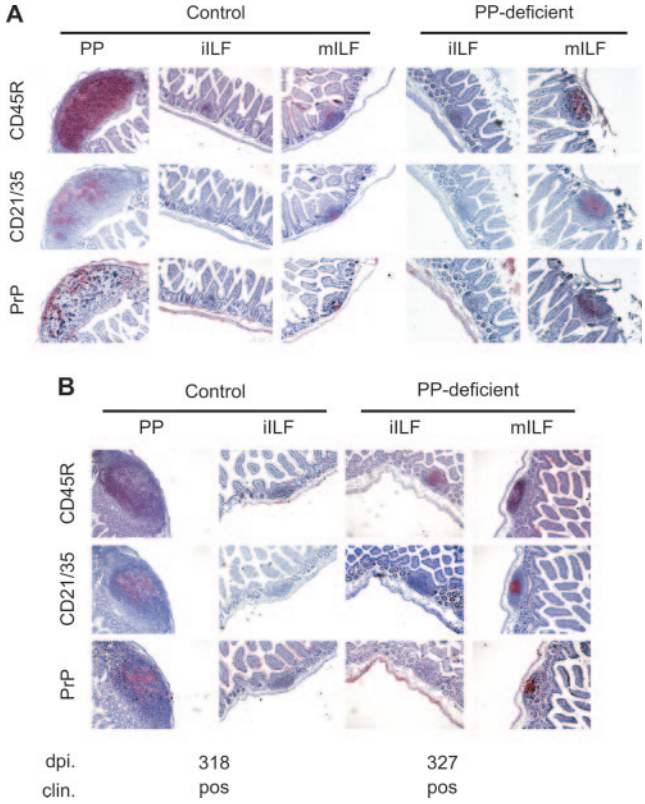

FIGURE 8. Detection of PrP^d in the intestines of control mice and PP-deficient mice following oral inoculation with the scrapie agent. Small intestines were collected (*A*) 70 days after oral inoculation or (*B*) at the terminal stage of disease. Adjacent sections were stained with CD45R-specific antiserum B220 to detect B lymphocytes (red), CD21/35-specific antiserum to detect CR2/CR1-expressing FDCs (red), and PrP-specific antiserum 1B3 (red). At each time point after scrapie inoculation, strong PrP^d staining was found to colocalize with CD21/35-expressing FDCs in the PPs and the mILFs of control mice and also in the mILFs of PP-deficient mice. dpi, day postinoculation on which the tissues were analyzed; pos, mice that developed clinical signs of scrapie; neg, mice that were free of the signs of scrapie. Original magnification: ×100.

maturation status. In this study, >1000 ILFs were analyzed, and our data showed that all mILFs consistently possessed large networks of immune complex-trapping FDCs (Fig. 7, *A* and *B*). FDCs were never detected in iILFs (Fig. 7, *A* and *C*). Like PPs, ILFs lack afferent lymphatics, but LYVE-1-expressing cells were observed in close association with ILFs, indicating the presence of efferent lymphatics (Fig. 7*E*). S-100-expressing nerve fibers and supportive cells were detected within the gut wall and in close association with mILFs (Fig. 7*F*).

Involvement of mILFs in scrapie agent neuroinvasion from the intestine

Having demonstrated that mILFs contain large FDC networks we next determined whether scrapie agent neuroinvasion from the intestine could also occur from mILFs. Stimulation via LTβR is also important for the development of ILFs as these structures are absent in LT-deficient mice (30, 36). However, unlike PPs, ILF formation occurs postnatally, and their development in LT-deficient

Table III. *Effect of PP deficiency on susceptibility to orally inoculated scrapie*

	Presence at Time of Inoculation					Oral Scrapie Inoculation	
Mice	PPs	mILFs[a]	MLNs	SPL	FDCs	Incidence	Mean incubation period (days) ± SE
C57BL/Dk (control)	+[b]	2	+	+	+	16/16	319 ± 3
PP deficient[c]	−	20	+	+	+	10/10	313 ± 6

[a] Number of mILFs present in the small intestine at the time of inoculation.
[b] +, present; −, absent.
[c] Mice treated in utero with LTβR-Ig on day 11.5 of gestation to ablate PP formation.

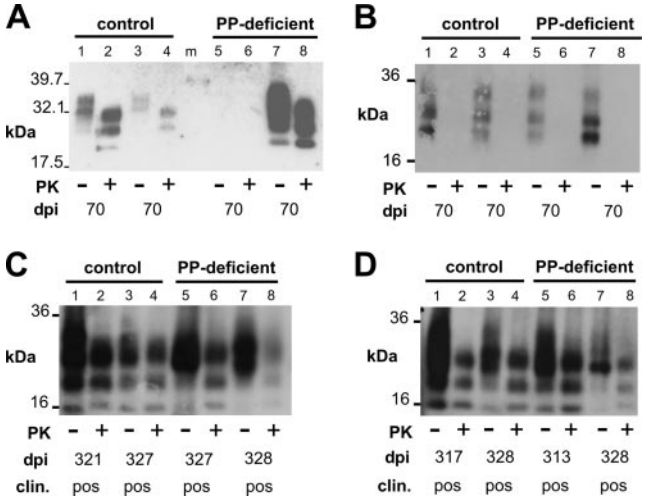

FIGURE 9. PrP^{Sc} accumulation in the MLNs and spleens of control mice and PP-deficient mice following oral inoculation with scrapie. MLNs (*A* and *C*) and spleens (*B* and *D*) were collected 70 days after oral inoculation with the scrapie agent (*A* and *B*) or at the terminal stage of disease (*C* and *D*). Samples were treated in the presence (+) or absence (−) of proteinase K (PK) before electrophoresis. *Lane M* contained molecular mass markers. dpi, day postinoculation on which the tissues were analyzed; pos, mice that developed clinical signs of scrapie; neg, mice that were free of the signs of scrapie.

mice can be restored by reconstitution with WT bone marrow (30, 36). In the experiments described above (Table II), no FDC-containing mILFs were present within the intestines of WT→WT mice, WT→LT$\alpha^{-/-}$ mice, and WT→LT$\beta^{-/-}$ mice at the time of scrapie inoculation, as these structures take much longer than 35 days to develop after WT bone marrow transfer (~8–12 wk; Refs. 30 and 37). The numbers of mILFs in the intestines of immunocompetent control mice in our specific pathogen-free colony are extremely low or absent (typically 0–6 mILFs/mouse). However, in the absence of PPs, LTβR stimulation substantially increases the number of mILFs in the intestine (30). We therefore created mice that lacked PPs but contained numerous mILFs in their intestines through treatment of pregnant C57BL/Dk mice with LTβR-Ig (26, 30). As expected, PP formation in the progeny mice was blocked (termed PP-deficient mice), but the development of a significantly greater number of FDC-containing mILFs was induced when compared with untreated C57BL/Dk (control) mice ($p \leq 0.001$; Table III).

Control and PP-deficient mice (81–110 days old) were inoculated orally with the scrapie agent. Strong accumulations of PrP^{d} were observed upon FDCs within each of the numerous mILFs of PP-deficient mice (~20 mILFs per PP-deficient mouse, $n = 14$) and the PPs and occasional mILFs in control mice within 70 days of oral inoculation (Fig. 8*A*) and at the terminal stage of disease (Fig. 8*B*). PrP^{d} accumulations were never observed within iILFs from each mouse group.

In the MLNs, PrP^{Sc} was detected in all tissues from control mice 70 days after inoculation, but the levels detected in tissues from PP-deficient mice were variable (Fig. 9*A*). However, high levels of PrP^{Sc} levels were detected in MLNs from each mouse group at the terminal stage of disease (Fig. 9*C*). No PrP^{Sc} was detected in any of the spleens taken from control mice and PP-deficient mice 70 days after inoculation (Fig. 9*B*), but strong accumulations were observed at the terminal stage of disease (Fig. 9*D*).

Additional experiments demonstrated that the susceptibility of PP-deficient mice to orally inoculated scrapie agent was not significantly affected, as all control mice and PP-deficient mice succumbed to clinical TSE disease with similar incubation periods (Table III) and displayed similar neuropathological characteristics within the brain (data not shown). Together, these data imply that FDCs within mILFs are also important sites of TSE agent neuroinvasion from the intestine.

Discussion

In this study, we show that in the combined absence of the GALT and FDCs at the time of inoculation, scrapie agent transmission from the gastrointestinal tract is blocked. Furthermore, when FDC maturation is induced in remaining lymphoid tissues, mice that lack PPs remain refractory to oral scrapie challenge. Although the scrapie agent also accumulates upon FDCs within the MLNs shortly after inoculation, our data show that MLNs are dispensable for TSE agent neuroinvasion from the intestine. We show that mILFs along the antimesenteric wall of the small intestine contain large FDC networks, and like PPs, are important sites of TSE agent neuroinvasion. Together, these data demonstrate that TSE agent accumulation upon FDCs within GALT in the intestine itself (e.g., PPs and mILFs) is critically required for efficient neuroinvasion following oral exposure.

When considered in the context of recent studies, our data suggest that TSE agent neuroinvasion from the intestine occurs via the following pathway. Following oral inoculation, FDCs are critical initial sites of TSE agent accumulation within the GALT (13). In the absence of FDCs at the time of inoculation, TSE agent accumulation in the PP and subsequent neuroinvasion are blocked (13). In the current study, we show that in the absence of PPs, but not FDCs within other lymphoid tissues, neuroinvasion is likewise blocked indicating a critical role for PPs and the FDCs within them in TSE agent neuroinvasion from the intestine. We also show that mILFs, like PPs, are novel and important sites of TSE agent neuroinvasion from the intestine. Because the number and maturation status of ILFs is dramatically influenced by luminal stimuli (30, 38, 39), our data suggest that the presence of mILFs will significantly affect TSE susceptibility. Although early TSE agent accumulation also occurs within the MLNs following oral inoculation, we demonstrate that their presence does not influence disease pathogenesis. Likewise, FDCs within the spleen were also unable to compensate for the absence of the PPs. Together these data imply that neuroinvasion most likely occurs directly from lymphoid tissue within the intestine following accumulation upon FDCs. This conclusion is congruent with data from an epidemiological, mathematical, and pathological study, which suggested that for sheep, cattle, and humans, there was an association between development of lymphoid tissues in the gastrointestinal tract and susceptibility to natural TSE infection (40). The precise role that FDCs play in TSE pathogenesis awaits definitive demonstration, but they appear to amplify the levels of the TSE agent above the threshold required to achieve neuroinvasion (11–14). When and how the TSE agent spreads from the FDCs within PPs to the peripheral nervous system is likewise unknown. FDC depletion 14 days after oral inoculation does not affect pathogenesis, implying that neuroinvasion occurs from a very early stage postexposure and before the agent has disseminated to other lymphoid tissues (13). We show that within mILFs, like PPs (19), FDC networks are situated in close association with the nerve fibers that run along the gut wall. As the distance between FDCs and peripheral nerves appears to modulate the rate of TSE agent neuroinvasion (16), it is likely that the close association of FDCs with the nerve fibers that run along the gut wall facilitates the rapid spread of the TSE agent from PPs and mILFs to neighboring enteric nerves. Indeed, studies have demonstrated that PrP^{d} accumulates within enteric ganglia soon after oral inoculation (19).

How TSE agents are initially acquired from the gut lumen and cross the intestinal epithelium is not known, but several mechanisms have been implicated including transcytosis by M cells (41)

and possibly also capture and transport by migratory bone marrow-derived dendritic cells (42). In the current study, any potential effects on dendritic cell migration to the spleen, due to a lack of $LT\alpha_1\beta_2$ expressing B lymphocytes (43), were restored by WT bone marrow reconstitution. However, our data cannot exclude the possibility that the lack of M cells within the follicle associated epithelia of $LT\alpha^{-/-}$ mice, $LT\beta^{-/-}$ mice, WT→$LT\alpha^{-/-}$ mice, and WT→$LT\beta^{-/-}$ mice at the time of inoculation also contributes to their resistance to orally inoculated scrapie agent.

The inability of the MLNs or spleen to compensate for the absence of the PPs is unlikely to be due to fundamental differences in the nature of the FDCs at each of these sites as no significant differences between the function of FDCs from these tissues has been described, and each population appears to express similar levels of PrP^c and CR1/CR2. Following oral inoculation, the TSE agent accumulates first in PPs and is subsequently distributed via the lymph and/or blood-stream to the MLNs and spleen (Ref. 13 and current study). In the absence of the PPs, our data show that this down-stream distribution is blocked.

Diet (e.g., consumption of TSE agent-contaminated food) and PrP genotype (44, 45) are important risk factors that affect TSE susceptibility, but others remain to be determined. Recent studies suggest that inflammation may be another factor, either enhancing agent uptake from mucosal sites (46), or expanding the tissue distribution of these agents (47–49). For example, the induction of FDC networks within the ectopic germinal centers of chronically inflamed kidneys enables the accumulation of high levels of PrP^{Sc} in this tissue and excretion of low levels of infectivity in urine (47, 48). Likewise, natural chronic inflammatory conditions can expand the deposition of PrP^{Sc} in TSE-affected animals, such as to inflamed mammary glands of scrapie-affected sheep (49).

ILFs are recently identified lymphoid structures distributed throughout the intestines of rodents (36, 50–52) and humans (53) with features similar to PPs. Although the small intestine of an adult mouse may contain as many as 100 ILFs, data from the current study and others (30, 37) show that mILFs are highly infrequent (typically <5 per mouse) in tissues from unmanipulated immunocompetent control mice in a specific pathogen-free colony. Stimulation via LTβR is also important for the development of ILFs, but unlike PPs, their formation occurs postnatally (30, 37). In response to exogenous stimuli, LT-expressing B lymphocytes trigger the progression of iILFs into mILFs resembling lymphoid nodules containing a single B lymphocyte follicle of predominantly B2-B lymphocytes with a germinal center and a follicle associated epithelium containing M cells (30, 37, 54). Our analysis also demonstrates that mILFs consistently contain large FDC networks, which are not present in iILFs. Because the inducible nature of mILFs (30, 38) shares features with the ectopically induced germinal centers described above (47–49) we reasoned that mILFs might represent an important novel site of TSE agent accumulation and neuroinvasion in the small intestine.

To specifically determine the potential involvement of mILFs in scrapie agent transmission from the gastrointestinal tract, temporary in utero blockade of the LTβR signaling pathway was used to create mice that lacked PPs (termed PP-deficient mice), but contained numerous mILFs (26, 30). Our experiments demonstrate that FDCs within mILFs are novel and important sites of TSE agent accumulation within the small intestine. Furthermore, due to the presence of a significantly larger number of FDC-containing mILFs in PP-deficient mice, disease susceptibility was unaffected by the absence of PPs. The formation and maturation status of ILFs can be modulated by both lumenal bacterial flora (30, 38) and pathogenic microorganisms (39), implying that the microbiological status of the intestine at the time of TSE agent exposure might dramatically enhance disease susceptibility.

In the current study, our animals eat the scrapie agent to model oral pathogenesis as closely as possible. Following ingestion of the scrapie agent many factors will act on the inoculum to aid its elimination from the host. Indeed, much of the inoculum will be eliminated from the host by factors including digestion (by enzymes secreted in the stomach or small intestine) and excretion. As a consequence, following oral inoculation very little of the original inoculum will be available to be translocated across the gut epithelium by M cells or other potential mechanisms (41, 42). In WT mice it is likely that once the remaining fraction of the inoculum enters the lamina propria a competitive state exists whereby cells such as macrophages aid the clearance of the TSE agent (55, 56), whereas FDCs act to expand the levels of the TSE agent above the threshold required to achieve neuroinvasion. Thus, in the absence of FDCs (and lymphoid tissue within the intestine) in LT-deficient mice, the residual fraction of the inoculum will be gradually destroyed by phagocytic cells (55, 56). We have previously shown that the temporary depletion of FDCs for ~21–28 days blocks TSE agent transmission from the intestine (13), suggesting this time interval is sufficient to allow clearance of the remaining inoculum. In the current study, no mILFs were detected in the small intestines of WT→$LT\alpha^{-/-}$ mice and WT→$LT\beta^{-/-}$ mice at the time the mice were inoculated with the scrapie agent (5 wk after bone marrow reconstitution) as their formation occurs between 8 and 12 wk after WT bone marrow reconstitution (30, 37). Therefore, by the time the mILFs had eventually developed in the intestines of WT→$LT\alpha^{-/-}$ mice and WT→$LT\beta^{-/-}$ mice, sufficient time will have elapsed to allow clearance of the remaining inoculum, preventing PrP^d accumulation upon the FDCs within them and subsequent neuroinvasion.

In conclusion, our data demonstrate the crucial importance of TSE agent accumulation upon FDCs within the GALT for efficient neuroinvasion following oral exposure. Current evidence suggests vCJD shares a similar requirement for accumulation upon FDCs before neuroinvasion (5). Thus, our data imply that neuroinvasion of the vCJD agent might also occur soon after accumulation within the GALT before the agent has disseminated to other lymphoid tissues. Our data also identify mILFs as a novel and important site of TSE agent accumulation within the small intestine. As the formation and maturation status of ILFs is strongly influenced by commensal and pathogenic microorganisms (30, 38, 39), factors that stimulate mILF development are likely to dramatically enhance susceptibility to orally acquired TSE agents.

Acknowledgments

We thank Karen Brown, Claudine Raymond, Simon Cumming, Rebecca Greenan, and Irene McConnell (Institute for Animal Health, Neuropathogenesis Unit, Edinburgh, U.K.) for excellent technical support; Christine Farquhar (Institute for Animal Health) for provision of pAb 1B3; and Man-Sun Sy (Case Western Reserve University School of Medicine, Cleveland, OH) for provision of 8H4 mAb. LTβR-Ig was provided by Jeffrey Browning (Biogen, Cambridge, MA), and requests for this reagent should be addressed to Jeff_Browning@biogen.com.

Disclosures

The authors have no financial conflict of interest.

References

1. Büeler, H., A. Aguzzi, A. Sailer, R.-A. Greiner, P. Autenried, M. Aguet, and C. Weissmann. 1993. Mice devoid of PrP are resistant to scrapie. *Cell* 73: 1339–1347.
2. Bolton, D. C., M. P. McKinley, and S. B. Prusiner. 1982. Identification of a protein that purifies with the scrapie prion. *Science* 218: 1309–1311.
3. van Keulen, L. J. M., B. E. C. Schreuder, R. H. Meloen, G. Mooij-Harkes, M. E. W. Vromans, and J. P. M. Langeveld. 1996. Immunohistological detection of prion protein in lymphoid tissues of sheep with natural scrapie. *J. Clin. Microbiol.* 34: 1228–1231.

4. Sigurdson, C. J., E. S. Williams, M. W. Miller, T. R. Spraker, K. I. O'Rourke, and E. A. Hoover. 1999. Oral transmission and early lymphoid tropism of chronic wasting disease PrP^{res} in mule deer fawns (*Odocoileus hemionus*). *J. Gen. Virol.* 80: 2757–2764.
5. Hilton, D., E. Fathers, P. Edwards, J. Ironside, and J. Zajicek. 1998. Prion immunoreactivity in appendix before clinical onset of variant Creutzfeldt-Jakob disease. *Lancet* 352: 703–704.
6. Andreoletti, O., P. Berthon, D. Marc, P. Sarradin, J. Grosclaude, L. van Keulen, F. Schelcher, J.-M. Elsen, and F. Lantier. 2000. Early accumulation of PrP^{Sc} in gut-associated lymphoid and nervous tissues of susceptible sheep from a Romanov flock with natural scrapie. *J. Gen. Virol.* 81: 3115–3126.
7. McBride, P., P. Eikelenboom, G. Kraal, H. Fraser, and M. E. Bruce. 1992. PrP protein is associated with follicular dendritic cells of spleens and lymph nodes in uninfected and scrapie-infected mice. *J. Pathol.* 168: 413–418.
8. Brown, K. L., K. Stewart, D. Ritchie, N. A. Mabbott, A. Williams, H. Fraser, W. I. Morrison, and M. E. Bruce. 1999. Scrapie replication in lymphoid tissues depends on PrP-expressing follicular dendritic cells. *Nat. Med.* 5: 1308–1312.
9. Mabbott, N. A., A. Williams, C. F. Farquhar, M. Pasparakis, G. Kollias, and M. E. Bruce. 2000. Tumor necrosis factor α-deficient, but not interleukin-6-deficient, mice resist peripheral infection with scrapie. *J. Virol.* 74: 3338–3344.
10. Kosco-Vilbois, M. H. 2003. Are follicular dendritic cells really good for nothing? *Nat. Rev. Immunol.* 3: 764–769.
11. Mabbott, N. A., F. Mackay, F. Minns, and M. E. Bruce. 2000. Temporary inactivation of follicular dendritic cells delays neuroinvasion of scrapie. *Nat. Med.* 6: 719–720.
12. Montrasio, F., R. Frigg, M. Glatzel, M. A. Klein, F. Mackay, A. Aguzzi, and C. Weissmann. 2000. Impaired prion replication in spleens of mice lacking functional follicular dendritic cells. *Science* 288: 1257–1259.
13. Mabbott, N. A., J. Young, I. McConnell, and M. E. Bruce. 2003. Follicular dendritic cell dedifferentiation by treatment with an inhibitor of the lymphotoxin pathway dramatically reduces scrapie susceptibility. *J. Virol.* 77: 6845–6854.
14. Mohan, J., M. E. Bruce, and N. A. Mabbott. 2005. Follicular dendritic cell dedifferentiation reduces scrapie susceptibility following inoculation via the skin. *Immunology* 114: 225–234.
15. Glatzel, M., F. L. Heppner, K. M. Albers, and A. Aguzzi. 2001. Sympathetic innervation of lymphoreticular organs is rate limiting for prion neuroinvasion. *Neuron* 31: 25–34.
16. Prinz, M., M. Heikenwalder, T. Junt, P. Schwarz, M. Glatzel, F. L. Heppner, Y.-X. Fu, M. Lipp, and A. Aguzzi. 2003. Positioning of follicular dendritic cells within the spleen controls prion neuroinvasion. *Nature* 425: 957–962.
17. Bruce, M. E., R. G. Will, J. W. Ironside, I. McConnell, D. Drummond, A. Suttie, L. McCardle, A. Chree, J. Hope, C. Birkett, et al. 1997. Transmissions to mice indicate that "new variant" CJD is caused by the BSE agent. *Nature* 389: 498–501.
18. Kimberlin, R. H., and C. A. Walker. 1989. Pathogenesis of scrapie in mice after intragastric infection. *Virus Res.* 12: 213–220.
19. Beekes, M., and P. A. McBride. 2000. Early accumulation of pathological PrP in the enteric nervous system and gut-associated lymphoid tissue of hamsters orally infected with scrapie. *Neurosci. Lett.* 278: 181–184.
20. Oldstone, M. B. A., R. Race, D. Thomas, H. Lewicki, D. Homman, S. Smelt, A. Holz, P. Koni, D. Lo, B. Chesebro, and R. Flavell. 2002. Lymphotoxin-α- and lymphotoxin-β-deficient mice differ in susceptibility to scrapie: evidence against dendritic cell involvement. *J. Virol.* 76: 4357–4363.
21. Prinz, M., G. Huber, A. J. S. Macpherson, F. L. Heppner, M. Glatzel, H.-P. Eugster, N. Wagner, and A. Aguzzi. 2003. Oral prion infection requires normal numbers of Peyer's patches but not of enteric lymphocytes. *Am. J. Pathol.* 162: 1103–1111.
22. Horiuchi, M., H. Furuoka, N. Kitamura, and M. Shinagawa. 2006. Alymphoplasia mice are resistant to prion infection via oral route. *Jpn. J. Vet. Res.* 53: 149–157.
23. Riminton, D. S., H. Körner, D. H. Strickland, F. A. Lemckert, J. D. Pollard, and J. D. Sedgwick. 1998. Challenging cytokine redundancy: inflammatory cell movement and clinical course of experimental autoimmune encephalomyelitis are normal in lymphotoxin-deficient, but not tumour necrosis factor-deficient, mice. *J. Exp. Med.* 187: 1517–1528.
24. Ngo, V. N., H. Korner, M. D. Gunn, K. N. Schmidt, D. S. Riminton, M. D. Cooper, J. L. Browning, J. D. Sedgwick, and J. G. Cyster. 1999. Lymphotoxin α/β and tumour necrosis factor are required for stromal cell expression of homing chemokines in B and T cell areas of the spleen. *J. Exp. Med.* 189: 403–412.
25. Force, W. R., B. N. Walter, C. Hession, R. Tizard, C. A. Kozak, J. L. Browning, and C. F. Ware. 1995. Mouse lymphotoxin-β receptor. *J. Immunol.* 155: 5280–5288.
26. Rennert, P. D., J. L. Browning, R. Mebius, F. Mackay, and P. S. Hochman. 1996. Surface lymphotoxin α/β complex is required for the development of peripheral lymphoid organs. *J. Exp. Med.* 184: 1999–2006.
27. Fraser, H., and A. G. Dickinson. 1973. Agent-strain differences in the distribution and intensity of grey matter vacuolation. *J. Comp. Pathol.* 83: 29–40.
28. Fraser, H., and A. G. Dickinson. 1968. The sequential development of the brain lesions of scrapie in three strains of mice. *J. Comp. Pathol.* 78: 301–311.
29. Farquhar, C. F., R. A. Somerville, and L. A. Ritchie. 1989. Post-mortem immunodiagnosis of scrapie and bovine spongiform encephalopathy. *J. Virol. Methods* 24: 215–222.
30. Lorenz, R. G., D. D. Chaplin, K. G. McDonald, J. S. McDonough, and R. D. Newberry. 2003. Isolated lymphoid follicle formation is inducible and dependent upon lymphotoxin-sufficient B lymphocytes, lymphotoxin β receptor, and TNF receptor 1 function. *J. Immunol.* 170: 5474–5482.
31. Wadsworth, J. D. F., S. Joiner, A. F. Hill, T. A. Campbell, M. Desbruslais, P. J. Luthert, and J. Collinge. 2001. Tissue distribution of protease resistant prion protein in variant Creutzfeldt-Jakob disease using a highly sensitive immunoblotting assay. *Lancet* 358: 171–180.
32. Zanusso, G., D. Liu, S. Ferrari, I. Hegyi, X. Yin, A. Aguzzi, S. Hornemann, S. Liemann, R. Glockshuber, J. C. Manson, et al. 1998. Prion protein expression in different species: analysis with a panel of new mAbs. *Proc. Natl. Acad. Sci. USA* 95: 8812–8816.
33. Koni, P. A., R. Sacca, P. Lawton, J. L. Browning, N. H. Ruddle, and R. A. Flavell. 1997. Distinct roles in lymphoid organogenesis for lymphotoxins α and β revealed in lymphotoxin β-deficient mice. *Immunity* 6: 491–500.
34. de Togni, P., J. Goellner, N. H. Ruddle, P. R. Streeter, A. Fick, S. Mariathasan, S. C. Smith, R. Carlson, L. P. Shornick, J. Strauss-Schoenberger, et al. 1994. Abnormal development of peripheral lymphoid organs in mice deficient in lymphotoxin. *Science* 264: 703–707.
35. Mackay, F., and J. L. Browning. 1998. Turning off follicular dendritic cells. *Nature* 395: 26–27.
36. Hamada, H., T. Hiroi, Y. Nishiyama, H. Takahashi, Y. Masunaga, S. Hachimura, S. Kaminogawa, H. Takahashi-Iwanaga, T. Iwanaga, H. Kiyono, et al. 2002. Identification of multiple isolated lymphoid follicles on the antimesenteric wall of the mouse small intestine. *J. Immunol.* 168: 57–64.
37. McDonald, K. G., J. S. McDonough, and R. D. Newberry. 2005. Adaptive immune responses are dispensable for isolated lymphoid follicle formation: antigen-naive, lymphotoxin-sufficient B lymphocytes drive the formation of mature isolated lymphoid follicles. *J. Immunol.* 174: 5720–5728.
38. Fagarasan, S., M. Muramatsu, K. Suzuki, H. Nagaokam, H. Hiai, and T. Honjo. 2002. Critical roles of activation-induced cytidine deaminase in the homeostasis of gut flora. *Science* 298: 1424–1427.
39. Little, M. C., L. V. Bell, L. J. Cliffe, and K. J. Else. 2005. The characterization of intraepithelial lymphocytes, lamina propria leukocytes, and isolated lymphoid follicles in the large intestine of mice infected with the intestinal nematode parasite *Trichuris muris*. *J. Immunol.* 175: 6713–6722.
40. St. Rose, S., N. Hunter, D. Matthews, J. Foster, M. E. Chase-Topping, L. E. B. Kruuk, D. J. Shaw, S. M. Rhind, R. G. Will, and M. E. J. Woolhouse. 2006. Comparative evidence for a link between Peyer's patch development and susceptibility to transmissible spongiform encephalopathies. *BMC Infect. Dis.* 6: 5.
41. Heppner, F. L., A. D. Christ, M. A. Klein, M. Prinz, M. Fried, J.-P. Kraehenbuhl, and A. Aguzzi. 2001. Transepithelial prion transport by M cells. *Nat. Med.* 7: 976–977.
42. Huang, F.-P., C. F. Farquhar, N. A. Mabbott, M. E. Bruce, and G. G. MacPherson. 2002. Migrating intestinal dendritic cells transport PrP^{Sc} from the gut. *J. Gen. Virol.* 83: 267–271.
43. Kabashima, K., T. A. Banks, K. M. Ansel, T. T. Lu, C. F. Ware, and J. G. Cyster. 2005. Intrinsic lymphotoxin-β receptor requirement for homeostasis of lymphoid tissue dendritic cells. *Immunity* 22: 439–450.
44. Wadsworth, J. D. F., E. A. Asante, M. Desbruslais, J. M. Linehan, S. Joiner, I. Gowland, J. Welch, L. Stone, S. E. Lloyd, A. F. Hill, et al. 2004. Human prion protein with valine 129 prevents expression of variant CJD phenotype. *Science* 306: 1793–1796.
45. Goldmann, W., N. Hunter, G. Smith, J. Foster, and J. Hope. 1994. PrP genotype and agent effects in scrapie: change in allelic interaction with different isolates of agent in sheep, a natural host of scrapie. *J. Gen. Virol.* 75: 989–995.
46. Thackray, A. M., A. N. McKenzie, M. A. Klein, A. Lauder, and R. Bujdoso. 2004. Accelerated prion disease in the absence of interleukin-10. *J. Virol.* 78: 13697–13707.
47. Heikenwalder, M., N. Zeller, H. Seeger, M. Prinz, P.-C. Klöhn, P. Schwarz, N. H. Ruddle, C. Weissmann, and A. Aguzzi. 2005. Chronic lymphocytic inflammation specifies the organ tropism of prions. *Science* 307: 1107–1110.
48. Seeger, H., M. Heikenwalder, N. Zeller, J. Kranich, P. Schwarz, A. Gaspert, B. Seifert, G. Miele, and A. Aguzzi. 2005. Coincident scrapie infection and nephritis lead to urinary prion excretion. *Science* 310: 324–326.
49. Ligios, C., C. Sigurdson, C. Santucciu, G. Carcassola, G. Manco, M. Basagni, C. Maestrale, M. G. Cancedda, L. Madau, and A. Aguzzi. 2005. PrPSc in mammary glands of sheep affected by scrapie and mastitis. *Nat. Med.* 11: 1137–1138.
50. Keren, D. F., P. S. Holt, H. H. Collins, P. Gemski, and S. B. Formal. 1978. The role of Peyer's patches in the local immune response of rabbit ileum to live bacteria. *J. Immunol.* 120: 1892–1896.
51. Hitotsumatsu, O., H. Hamada, M. Naganuma, N. Inoue, H. Ishii, T. Hibi, and H. Ishikawa. 2005. Identification and characterisation of novel gut-associated lymphoid tissues in rat small intestine. *J. Gastroenterol.* 40: 956–963.
52. Rosner, A. J., and D. F. Keren. 1984. Demonstration of M cells in the specialized follicle-associated epithelium overlying isolated lymphoid follicles in the gut. *J. Leukocyte Biol.* 35: 397–404.
53. Moghaddami, M., A. Cummins, and G. Mayrhofer. 1998. Lymphocyte-filled villi: comparison with other lymphoid aggregations in the mucosa of the human small intestine. *Gastroenterology* 115: 1414–1425.
54. Shikina, T., T. Hiroi, K. Iwatani, M. H. Jang, S. Fukuyama, M. Tamura, T. Kubo, H. Ishikawa, and H. Kiyono. 2004. IgA class switch occurs in the organized nasopharynx- and gut-associated lymphoid tissue, but not in the diffuse lamina propria or airways and gut. *J. Immunol.* 172: 6259–6264.
55. Carp, R. I., and S. M. Callahan. 1982. Effect of mouse peritoneal macrophages on scrapie infectivity during extended in vitro incubation. *Intervirology* 17: 201–207.
56. Maignien, T., M. Shakweh, P. Calvo, D. Marcé, N. Salès, E. Fattal, J. P. Deslys, P. Couvreur, and C. I. Lasmézas. 2005. Role of gut macrophages in mice orally contaminated with scrapie or BSE. *Int. J. Pharm.* 298: 293–304.